Contents lists available at ScienceDirect

# Journal of Ginseng Research

Research Article

# Gypenoside XVII protects against myocardial ischemia and reperfusion injury by inhibiting ER stress–induced mitochondrial injury

Yingli Yu [a,b,c,d], Min Wang [a,b,c,d], Rongchang Chen [a,b,c,d], Xiao Sun [a,b,c,d], Guibo Sun [a,b,c,d,**], iaobo Sun [a,b,c,d,*]

[a] Beijing Key Laboratory of Innovative Drug Discovery of Traditional Chinese Medicine (Natural Medicine) and Translational Medicine, Institute of Medicinal Plant Development, Peking Union Medical College and Chinese Academy of Medical Sciences, Beijing, China
[b] Key Laboratory of Bioactive Substances and Resource Utilization of Chinese Herbal Medicine, Ministry of Education, Beijing, China
[c] Key Laboratory of new drug discovery based on Classic Chinese medicine prescription, Chinese Academy of Medical Sciences, Beijing, China
[d] Key Laboratory of the efficacy evaluation of Chinese Medicine against glycolipid metabolism disorder disease, State Administration of Traditional Chinese Medicine, Beijing, China

## ARTICLE INFO

## ABSTRACT

Background: Effective strategies are dramatically needed to prevent and improve the recovery from myocardial ischemia and reperfusion (I/R) injury. Direct interactions between the mitochondria and endoplasmic reticulum (ER) during heart diseases have been recently investigated. This study was designed to explore the cardioprotective effects of gypenoside XVII (GP-17) against I/R injury. The roles of ER stress, mitochondrial injury, and their crosstalk within I/R injury and in GP-17–induced cardioprotection are also explored.
Methods: Cardiac contractility function was recorded in Langendorff-perfused rat hearts. The effects of GP-17 on mitochondrial function including mitochondrial permeability transition pore opening, reactive oxygen species production, and respiratory function were determined using fluorescence detection kits on mitochondria isolated from the rat hearts. H9c2 cardiomyocytes were used to explore the effects of GP-17 on hypoxia/reoxygenation.
Results: We found that GP-17 inhibits myocardial apoptosis, reduces cardiac dysfunction, and improves contractile recovery in rat hearts. Our results also demonstrate that apoptosis induced by I/R is predominantly mediated by ER stress and associated with mitochondrial injury. Moreover, the cardioprotective effects of GP-17 are controlled by the PI3K/AKT and P38 signaling pathways.
Conclusion: GP-17 inhibits I/R-induced mitochondrial injury by delaying the onset of ER stress through the PI3K/AKT and P38 signaling pathways.

## 1. Introduction

Coronary artery diseases and associated ischemic heart diseases are prevalent worldwide [1]. The mechanisms underlying myocardial ischemic/reperfusion (I/R) injury are multifactorial [2,3]. We have previously demonstrated the occurrence of endoplasmic reticulum (ER) stress in I/R injury and shown that ER stress inhibition protects hearts from I/R injury [4]. Multiple mechanisms involving caspases, $Ca^{2+}$, Bcl-2 family proteins, and transcription factors link ER stress and apoptosis during I/R injury [5–7]. ER stress blocks mitochondrial $Ca^{2+}$ uptake, alters oxidative phosphorylation, and injures metabolic remodeling, thus impairing energy metabolism during many cardiac diseases [8]. Mitochondrial dysfunction, particularly mitochondrial permeability

transition pore (mPTP) opening, is destructive in heart injury [9,10]. mPTP reportedly remains closed during ischemia but opens in reperfusion [11]. Therefore, the mitochondria are a potential drug target for the treatment of I/R injury.

In our previous studies, gypenosides from *Panax notoginseng (Burk.)F. H. Chen* provided protective effects on cerebral vascular and cardiovascular diseases [4,12,13]. Gypenoside XVII (GP-17) (Fig. 1A) is derived from *Panax notoginseng* (Burk.). Previous studies have illustrated that GP-17 exerts neuroprotective effects against Aβ25−35− induced apoptosis in PC12 cells [14]. Gypenosides also protect against cerebral ischemia and show neuroprotective effects against oxidative injury [15]. Based on these previous reports, we were inspired to explore whether GP-17 provides cardioprotective effects against I/R injury and whether such protective effects are associated with ER stress− or mitochondrial injury−associated signaling pathways.

In this study, we explored the effects of GP-17 against I/R injury in Langendorff-perfused rat hearts and in I/R-treated H9c2 cells. Our results suggested that GP-17 reduced cardiac dysfunction, inhibited myocardial oxidative stress and apoptosis, and improved contractile recovery after I/R *ex vivo* and *in vitro*. We demonstrated that GP-17 protected against I/R-induced mitochondrial impairment by delaying the onset of ER stress through the PI3K/AKT and P38 signaling pathways.

## 2. Materials and methods

### 2.1. Materials

GP-17 (purity > 98%) was obtained from Shanghai Winherb Medical S&T Development (Shanghai, China). The cell culture
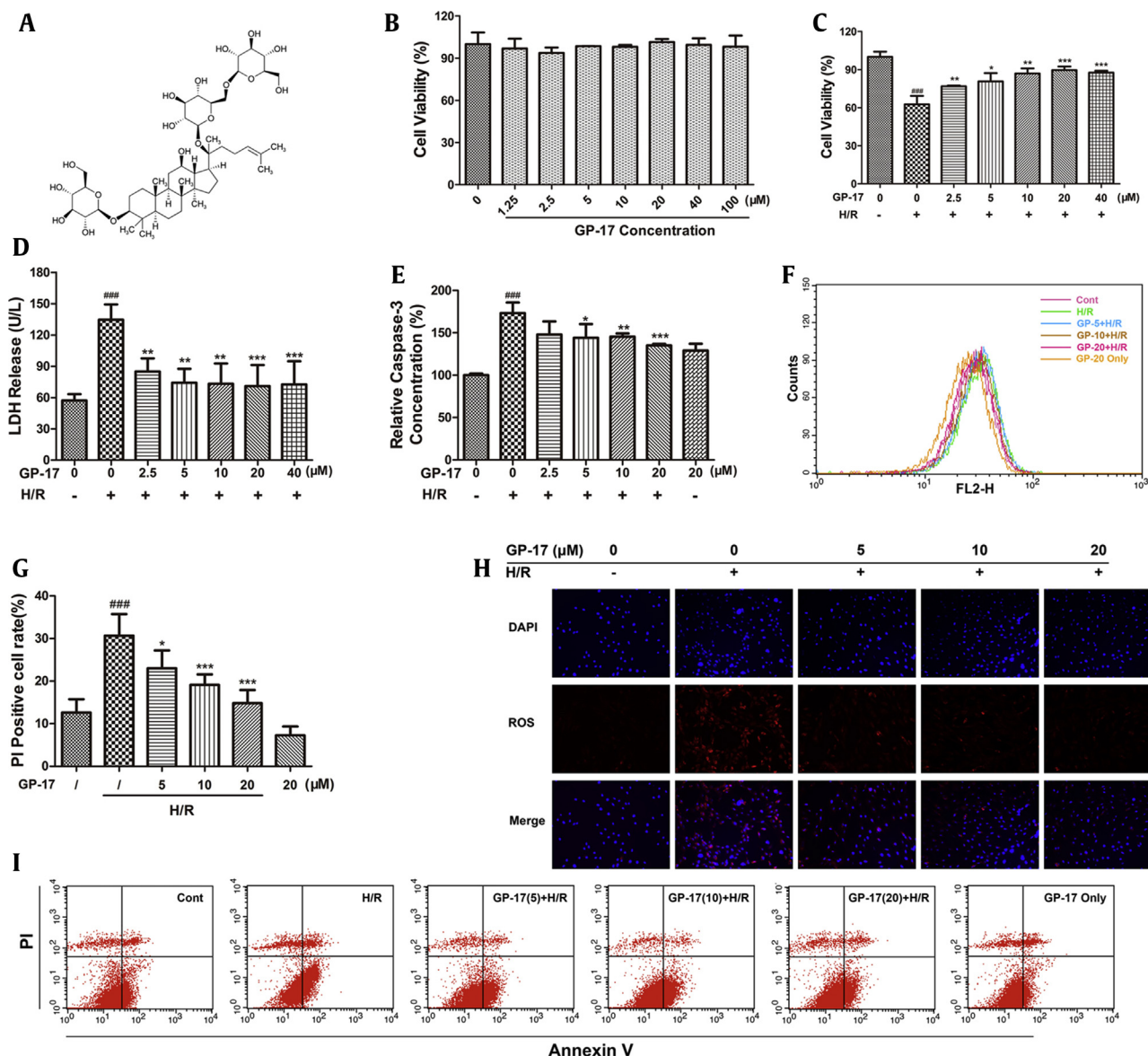


**Fig. 1.** Effects of GP-17 on H/R-processed H9c2 cardiomyocyte. H9c2 cardiomyocyte were incubated with different concentration of GP-17 for 24 h, followed by hypoxia for 6 h and reoxygenation for 12 h. (A) Chemical structure of GP-17; (B) GP-17 had no significant effects on cell viability with the concentration under 100 μM; (C) effects of GP-17 on H/R-induced cell death detected by CCK-8; (D) effects of GP-17 on H/R-induced LDH release and (E) caspase-3 activities; (F) ROS levels evaluated by a FACSCalibur flow cytometer; (G) the quantitative data of PI-positive cell rate compared with the control showed by bar diagram; (H) representative images of intracellular ROS-positive cells and merge; (I) the representative images of annexin V-(fluorescein isothiocyanate) FITC−positive cells or PI-positive cells. ###$P < 0.001$ versus the control, *$P < 0.05$ versus the I/R group, **$P < 0.01$ versus the I/R group, ***$P < 0.001$ versus the I/R group.

GP-17, gypenoside XVII; H/R, hypoxia/reoxygenation; CCK-8, cell counting kit-8; LDH, lactate dehydrogenase; ROS, reactive oxygen species; PI, propidium iodide.

materials, including fetal bovine serum, Dulbecco's modified Eagle's medium, and penicillin/streptomycin, were obtained from Gibco (NY, USA). The compounds used in Krebs-Henseleit (KH) buffer were purchased from Sigma-Aldrich Chemicals. The kits of malondialdehyde (MDA), catalase (CAT), lactate dehydrogenase (LDH), glutathione peroxidase (GSH-Px), and superoxide dismutase (SOD) were purchased from Jiancheng Bioengineering Institute (Nanjing, China). The primary antibodies, PI3K, P-PI3K, AKT, P-AKT, P38, P–P38, GRP78, P-PERK, PERK, P-eIf2α, eIf2α, ATF6, IRE1, P-JNK, JNK, CHOP, caspase-12, BAX, Bcl-2, BAD, and GAPDH were supplied by Santa Cruz Biotechnology (CA, USA).

## 2.2. H9c2 cell culture and hypoxia/reoxygenation

H9c2 cardiomyocytes were plated and grown in a humidified incubator at 37°C for at least 24 h containing 5% $CO_2$. For hypoxia/reoxygenation (H/R) processes, cells suffered 6 h of hypoxia and 12 h of reoxygenation as previously described [4]. Briefly, cells were removed to an anaerobic glove box (Coy Laboratory, USA), in which 5% $CO_2$ was changed to a combination of 5% $H_2$, 5% $CO_2$, and 90% $N_2$. After 6 h of hypoxia, cells were maintained in the regular incubator for 12 h as reperfusion.

## 2.3. Cell viability, lactate dehydrogenase leakage, and caspase-3 assay

The cell counting kit-8 (CCK-8, Dojindo, Kumamoto, Japan) was used to determine cell viability. 10 μl/well of CCK-8 solution was added to the cells cultured in 96-well plates ($5 \times 10^4$ cells/well) and kept in 37 °C for 4 h. The absorbance at 450 nm was detected by a microplate reader, and the cell viability was presented by the percentage of CCK-8 reduction relative to that of control. The culture medium was collected and analyzed by LDH assay according to the instructions.

A Fluorometric Assay Kit (BioVision, USA) was used to assess caspase-3 activity. Briefly, the lysed cells were centrifuged, and the supernatant was added by the caspase-3 substrate. Results were read by a Fluoroskan Ascent FL fluorometer (Thermo Fisher Scientific, USA) using a 400 nm excitation filter and 505 nm emission filter.

## 2.4. Reactive oxygen species production

Cells were separated by tryptic digestion and incubated in the dark at 37 °C with 25 μM of carboxy-H2DCFDA (Life Technologies, USA) for 30 min. FACSCalibur flow cytometer (BD Biosciences, CA, USA) was used to analyze the fluorescence. Images of the stained cells were immediately obtained using a high-content imaging system (Molecular Devices, USA).

## 2.5. Mitochondrial transmembrane potential (ΔΨm) and flow cytometry analysis

After preconditioning with GP-17 for 24 h and H/R treatment, cells were added by 2 μM of JC-1 and kept in the dark for 15 min at 37 °C as previously reported [12]. The labeled cell images were observed by ImageXpress Micro. Flow cytometry was used to assess cell apoptosis. $1 \times 10^6$ cells were incubated in the dark for 20 min with annexin V/propidium iodide (PI), resuspended in 300 ml binding buffer, and analyzed by FACScan flow cytometer within 1 h.

## 2.6. Oxygen consumption rate measured by Seahorse XF24 Analyzer

$2 \times 10^4$ cells were plated in quadruplicate wells of 24-well cell culture plates (Seahorse Bioscience, North Billerica, MA) and exposed to 20 μM of GP-17 with or without H/R. Then, the medium was replaced by the XF Assay Medium, which was added by 1 mM sodium pyruvate, 2 mM glutamine, and 0.9% glucose. After incubated in a non-$CO_2$ incubator for 1 h, we used the Seahorse Bioscience XF24 Extracellular Flux Analyzer (Seahorse Bioscience) to measure the oxygen consumption rate (OCR). The cells were added as the following: (1): basal levels were measured with no additives; (2) 1 μM OLIGO; (3) 0.3 μM FCCP; (4) 0.1 μM ROT. Both of the OCR (in pmol $O_2$/min) and pH change or absolute levels of $O_2$ and pH were visualized in the data output.

## 2.7. Animals and the langendorff procedure

Eight-week-old male SD rats (SCXK 2014-0001) weighing 200–220 g were purchased from Beijing Vital River Laboratory Animal Technology Co., Ltd. (Beijing, China). The animals were housed at $22 \pm 2°C$ with $60\% \pm 10\%$ humidity and light from 6:00–18:00 h for a 1-week acclimation period.

Heart function was assessed using the ADInstruments PowerLab system (ADInstruments, Sydney, Australia). The hearts were first perfused and equilibrated with KH buffer (11 mM glucose, 118 mM NaCl, 25 mM NaHCO₃, 4.8 mM KCl, 1.2 mM KH₂PO₄, 1.2 mM CaCl₂, 1.7 mM MgSO₄, and 0.7 mM Na pyruvate saturated with 95% $O_2$–5% $CO_2$ at 37°C, pH 7.4) for 15 min. Ranolazine 2-HCl (RaH), a late sodium channel blocker used for chronic stable angina treatment [16], was used as a positive control. GP-17 (dissolved in 5, 10, or 20 μM KH buffer) or RaH (dissolved in 0.3 mM KH buffer) were added 15 min before I/R treatment. For I/R treatment, the hearts were subjected to 40 min of global ischemia and 60 min of reperfusion. Similar doses of drugs were used for all experiments, some of which were performed with either GP-17 or RaH but not both. During the experiments, the following parameters were recorded continuously by a computerized Biopac system (California, USA): left ventricular systolic pressure (LVSP), left ventricular end-diastolic pressure (LVeDP), heart rate (HR), and maximum rate of left ventricular pressure development (+dP/dt$_{max}$) and decline (−dP/dt$_{min}$). The rats were randomly divided into the following groups of 12 rats each (1): control group (2); I/R group, in which 0.1% DMSO was added to the perfusate for 15 min and then global ischemia was carried out for 40 min and reperfusion for 60 min; (3, 4, and 5) GP-17 + I/R groups, in which the hearts were perfused with KH buffer dissolved with 5, 10, or 20 μM GP-17, respectively, for 15 min and then were subjected to global ischemia for 40 min followed by reperfusion; (6) GP-17 group, in which 20 μM GP-17 was added to the perfusate for 15 min and then replaced by pure perfusate for an additional 100 min; (7) RaH + I/R group, which is similar to the GP-17 + I/R groups but GP-17 was replaced by 0.3 mM RaH.

## 2.8. Heart histopathological examination, TUNEL staining, and antioxidant indices

The isolated rat hearts were fixed by 4% paraformaldehyde, and the left ventricles were dissected and embedded in paraffin blocks. Then, the blocks were sectioned, stained with hematoxylin and eosin, and examined by a pathologist blinded to the groups under a light microscope (170 Olympus, Tokyo, Japan).

The tissue slices were hydrated in ethanol and washed in double-distilled water. Terminal-deoxynucleoitidyl Transferase/(TdT-) Mediated Nick End Labeling (TUNEL) assay was performed according to the manufacturer's instructions (Roche Applied Science, Quebec, Canada). After incubation with Terminal-deoxynucleoitidyl Transferase (TdT) for 1 hour and hand washing in Phosphate-Buffered Saline (PBS), the slices were examined by using a fluorescence microscope.

The heart tissues were homogenized (10% w/v) in phosphate buffer (pH 7.4) and centrifuged. The activities of SOD, GSH-Px,
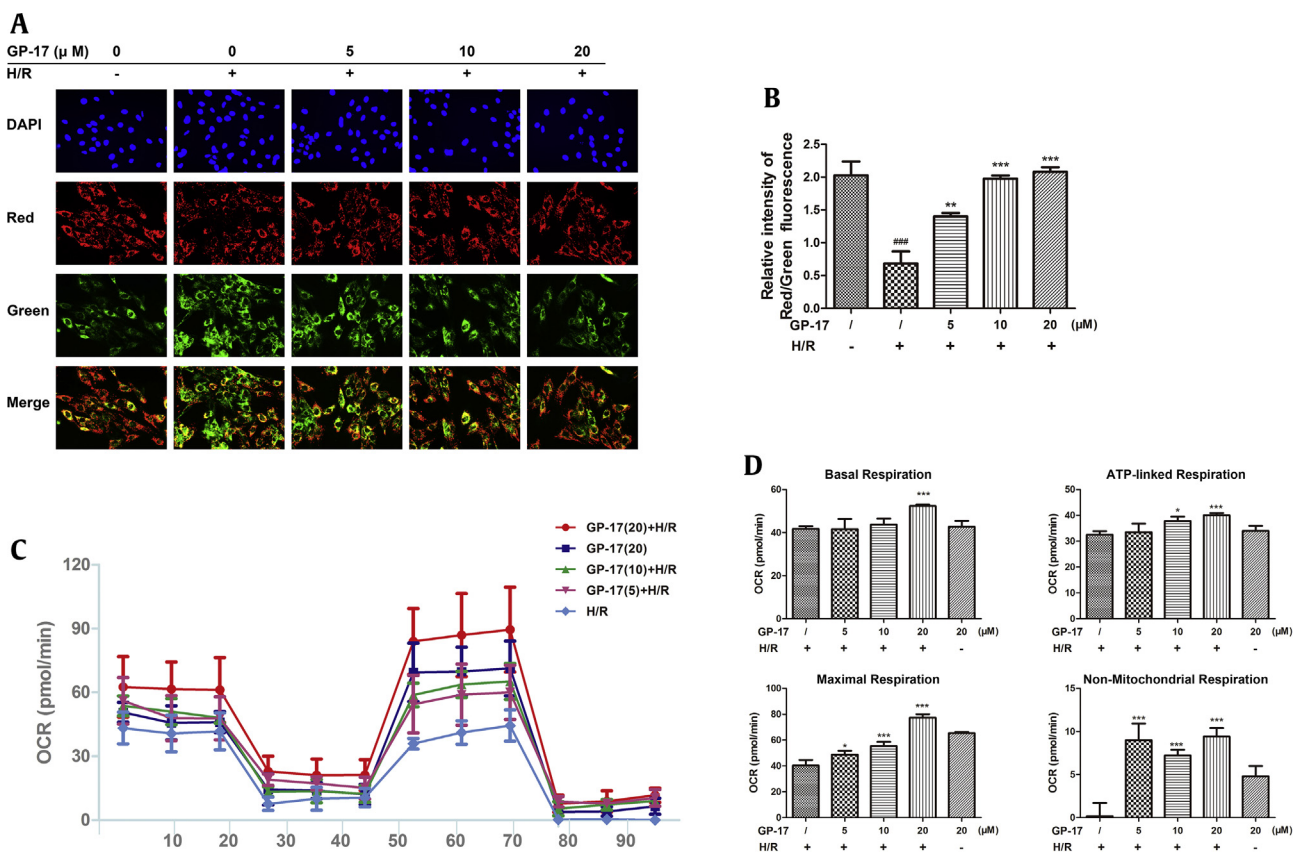
**Fig. 2.** Effects of GP-17 on depolarization of mitochondrial membrane and mitochondrial respiratory impairment induced by H/R. (A) Representative images showing JC-1 red or green cells and merge; (B) bar diagram of the red/green cells rate; (C) Seahorse XF24 mitochondrial stress analysis. (D) Bar diagrams showing the mitochondrial respiratory impairment measured by Seahorse XF24 analysis. $^{###}P < 0.001$ versus the control, $^{*}P < 0.05$ versus the I/R group, $^{**}P < 0.01$ versus the I/R group, $^{***}P < 0.001$ versus the I/R group. GP-17, gypenoside XVII; OCR, oxygen consumption rate.

and CAT and the content of MDA were measured in the supernatant.

### 2.9. Isolation of cardiac mitochondria and evaluation of mPTP opening, ROS concentration, mitochondrial calcium uptake, and mitochondrial calcium-ATP enzyme activity

After perfusion, the excised hearts were immediately placed on ice-cold isolation buffer that was supplemented with 250 mM sucrose, 5 mM Tris, and 1 mM EGTA. The ventricular tissue was minced and homogenized in isolation buffer (10 × the weight of tissue; Beyotime, Shanghai, China). After centrifuging at 600 g for 5 min, the sediment was resuspended in pancreatin on ice for an additional 20 min. After centrifugation at 11,000 g for 10 min, the pellets were resuspended in isolation buffer (without EGTA). This step was repeated once more. Then, mitochondrial protein concentrations were determined using Coomassie Brilliant Blue G reaction (Beyotime Biotechnology, Shanghai, China).

The mitochondria were loaded with increasing concentrations of $Ca^{2+}$ until the threshold was reached. The mitochondria underwent rapid $Ca^{2+}$ release because of mPTP opening as previously described [17]. The mPTP fluorescence detection kit (GenMed INC., Shanghai, China) using calcein-fluorescent staining was used to assess mPTP opening. Isolated mitochondria were stained with CM-

H2DCFDA (GenMed Scientifics INC., Shanghai, China), and changes in the dihydrodichlorofluorescein (DCF) fluorescence intensity were detected to measure reactive oxygen species (ROS) levels using a microplate reader (TECAN Infinite M1000, Austria). Mitochondrial calcium uptake was also measured (Genmed Scientifics INC., Shanghai, China). Each result was obtained using mitochondria isolated from the hearts of six different animals.

### 2.10. Real-time RT-PCR

RNA was extracted from the left ventricle of hearts by TRIzol reagent (Invitrogen Life Technologies, Carlsbad, CA, USA) and a total of 2μg RNA was reverse-transcribed into cDNA. The real-time PCR was conducted by Power SYBR Green PCR Master Mix (Applied Biosystems, Foster City, CA) in an iQ5 Real-time PCR detection system, and the cycle number was normalized to the GAPDH gene.

Primers: Grp78-F, GGAGGATGTGGGCACGGTGGTC, Grp78-R, GTCATTCCAAGTGCGTCCGATGAGG, GAPDH-F, GCGCCTGGTCAC-CAGGGCTGCTT, GAPDH-R, TGCCGAAGTGGTCGTGGATGACCT.

### 2.11. Western blot analysis

Total soluble protein of the left ventricle and cell samples were extracted by extraction buffer with 1 mM PMSF (Sigma). Equal amount of proteins was separated by the sodium dodecyl sulfate
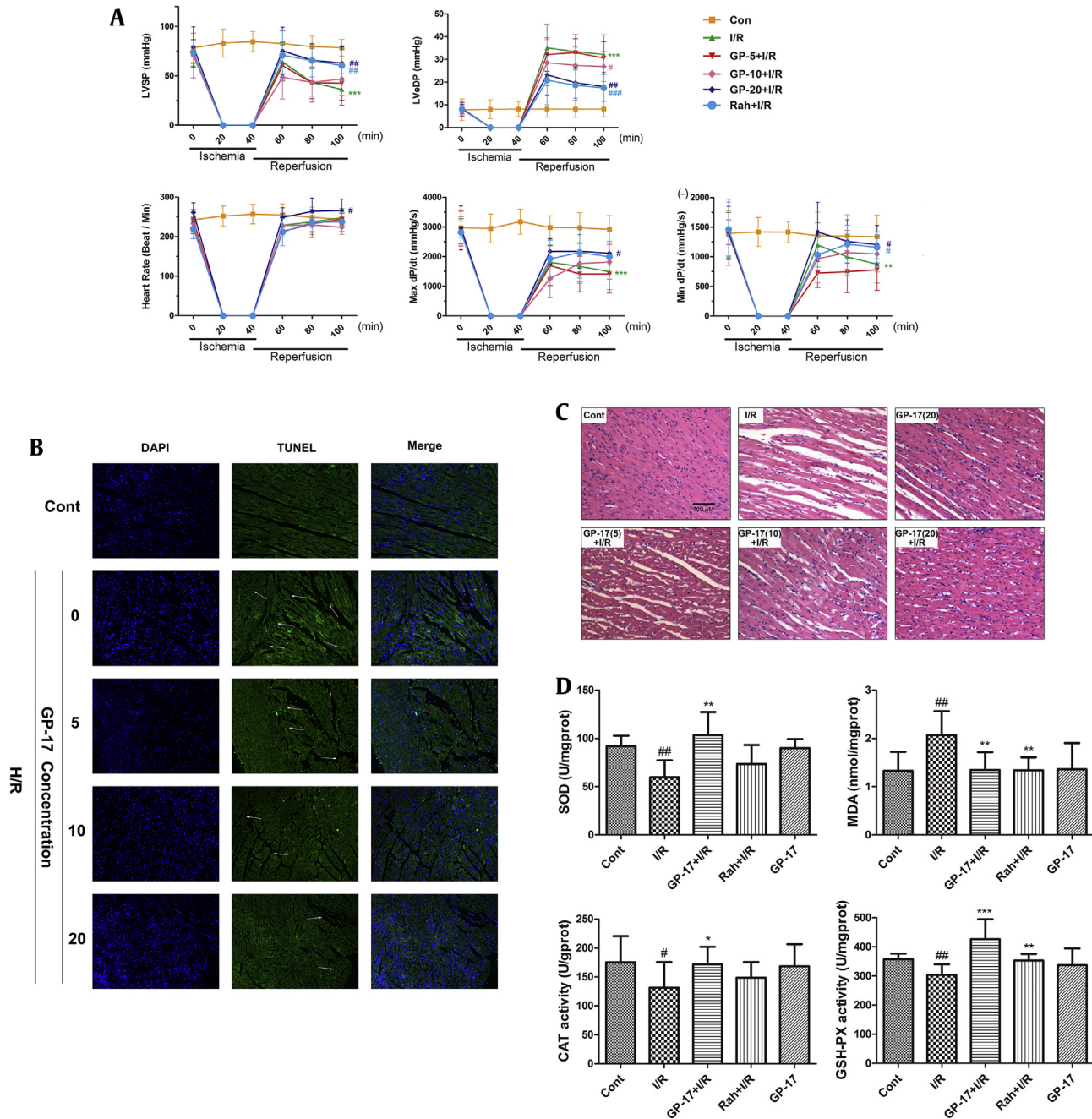
**Fig. 3.** Effects of GP-17 on heart dysfunction induced by I/R in the isolated rat hearts. (A) The real-time data of GP-17 on improving heart LVSP, LVeDP, heart rate, $+dp/dt_{max}$, and $-dp/dt_{min}$ in the Langendorff-perfused rat hearts; (B) histopathological examination showed GP-17's cardioprotection on I/R-impaired hearts; (C) the images of green fluorescent color showed TUNEL-positive nuclei or blue showed DAPI; (D) intracellular antioxidant enzyme activities examined by SOD, MDA, CAT, and GSH-Px. $^{#}P < 0.05$ versus the control, $^{##}P < 0.01$ versus the control, $^{*}P < 0.05$ versus the I/R group, $^{**}P < 0.01$ versus the I/R group, $^{***}P < 0.001$ versus the I/R group. GP-17, gypenoside XVII; I/R, ischemia and reperfusion; LVSP, left ventricular systolic pressure; LVeDP, left ventricular end-diastolic pressure; SOD, superoxide dismutase; MDA, malondialdehyde; CAT, catalase; GSH-Px, glutathione peroxidase.

polyacrylamide gel electrophoresis (SDS-PAGE) and then transferred to nitrocellulose membranes to be immunoblot-analyzed. After incubating with corresponding primary antibodies overnight, the membranes were then treated with secondary antibody of 1:1000 dilution conjugated with horseradish peroxidase. Molecular Devices densitometer (USA) and ImageJ software were used to determine the intensities of bands. GAPDH was used as an internal standard.

## 2.12. Statistical analysis

All the results are presented as mean ± SD from three independent experiments. One-way analysis of variance followed by Student-Newman-Keuls post hoc test was used to analyze the differences between the groups. $P < 0.05$ was considered statistically significant.
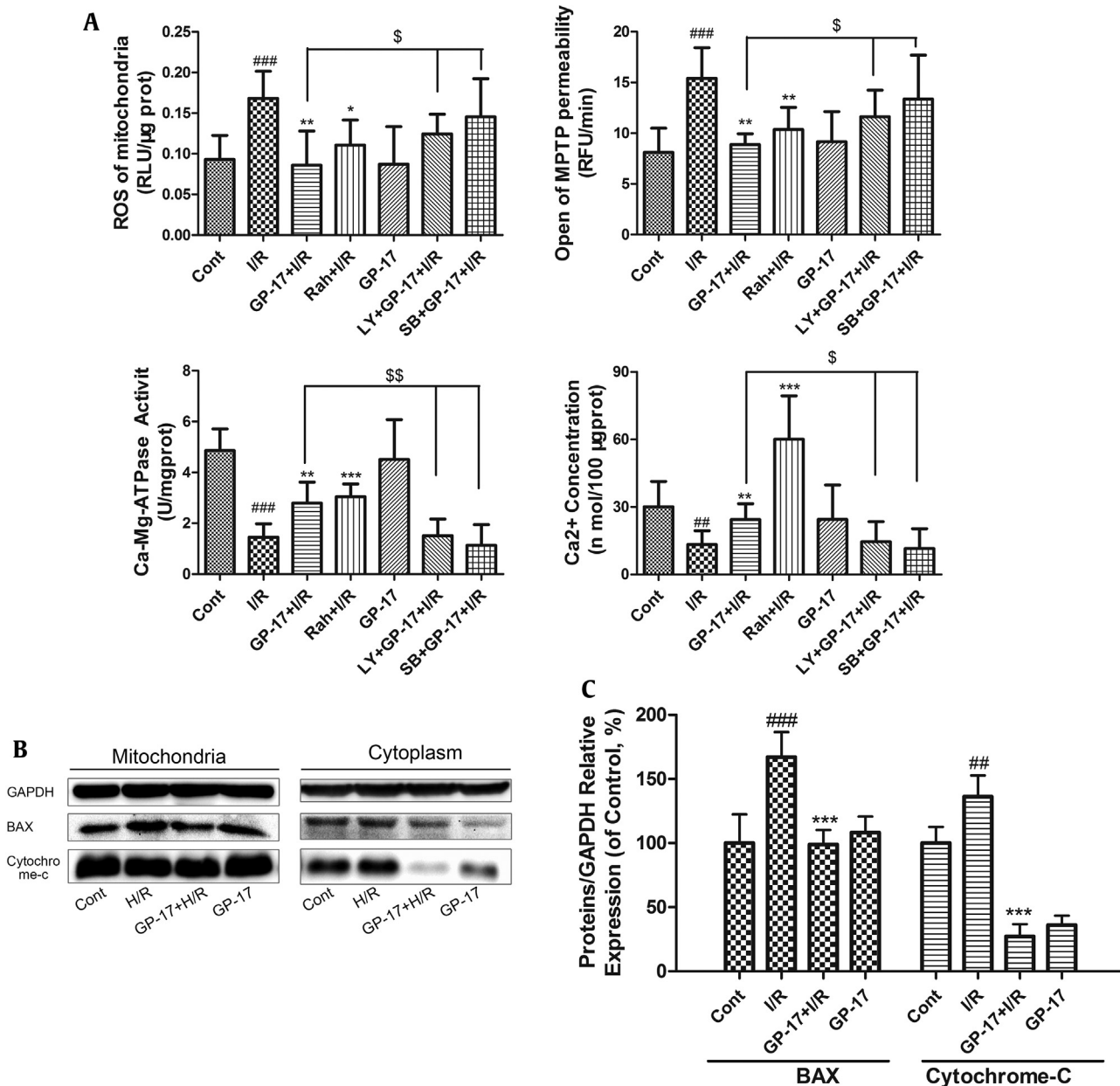
**Fig. 4.** Effects of GP-17 on mitochondrial damage induced by I/R in the isolated rat hearts. The mitochondria of the isolated rat hearts were extracted and detected by (A) ROS, opening of mPTP, Ca-ATPase, and $Ca^{2+}$ concentration; (B) immunoblot analysis of the protein levels in mitochondria and in cytoplasm; (C) bar graphs showing the relative protein expression. ##$P < 0.01$ versus the control, ###$P < 0.01$ versus the control, *$P < 0.05$ versus the I/R group, **$P < 0.01$ versus the I/R group, ***$P < 0.001$ versus the I/R group, $$P < 0.05$ versus GP-17 (20 μM)+ I/R group, $$$ P $< 0.01$ versus GP-17 (20 μM)+ I/R group.
GP-17, gypenoside XVII; I/R, ischemia and reperfusion; ROS, reactive oxygen species; mPTP, mitochondrial permeability transition pore.

### 2.13. Ethics statement

The animal experiments were under the regulations of the Chinese Guide for the Care and Use of Laboratory Animals.

## 3. Results

### 3.1. GP-17 protects H9c2 cells from H/R-induced cell death, LDH release, and caspase-3 activation

Fig. 1B shows that the cell viability of H9c2 cells was not significantly different between the GP-17 (1.25–100 μM)–treated groups and the control group ($P > 0.05$). Hypoxia treatment for 6 h

and reoxygenation for 12 h reduced the cell viability to approximately 60% compared with that in the control group (Fig. 1C, $P < 0.001$). This reduction was suppressed by GP-17 in a dose-dependent manner (2.5, 5, 10, and 20 μM) (Fig. 1C, $P < 0.05$, $P < 0.01$, or $P < 0.001$). The H/R treatment also increased LDH leakage from $57 \pm 6.2$ to $135 \pm 14.7$ compared with the control group, whereas GP-17 preconditioning significantly decreased LDH release (Fig. 1D, $P < 0.01$ or $P < 0.001$). Similar results were obtained in the caspase-3 analysis (Fig. 1E). Caspase-3 is an important component of the final pathway leading to cell apoptosis. As illustrated in Fig. 1E, H/R treatment increased the caspase-3 activity 1.73-fold compared with the control group ($P < 0.01$); in contrast, GP-17 significantly reduced the level of caspase-3 in a dose-
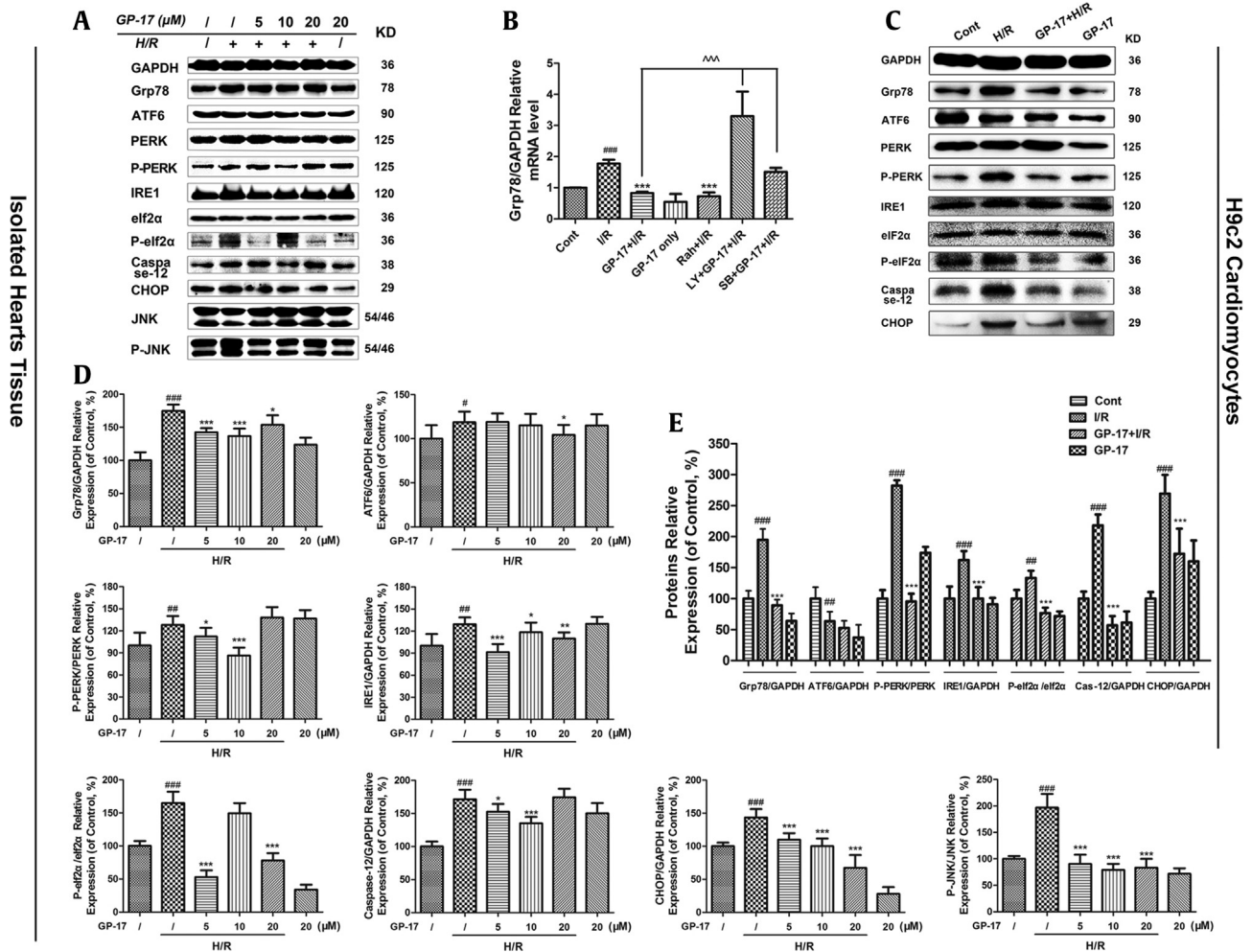
**Fig. 5.** Effects of GP-17 or I/R on the protein expression levels of UPR pathways and ER stress−associated apoptosis pathways. Expression levels of ER stress, UPR pathway protein, and the ER stress−associated apoptosis proteins were detected in the (A) isolated hearts and in (C) H9c2 cells; (B) the relative expression of Grp78 was detected by PCR; the relative expression levels of protein from isolated hearts (D) and from H9c2 cardiomyocytes (E) were expressed in the bar graphs. $^{\#}P < 0.05$ versus the control, $^{\#\#}P < 0.01$ versus the control, $^{\#\#\#}P < 0.001$ versus the control, $^{*}P < 0.05$ versus the I/R group, $^{**}P < 0.01$ versus the I/R, $^{***}P < 0.001$ versus the I/R, $^{\wedge\wedge\wedge}P < 0.001$ versus GP-17 (20 μM)+ I/R group. GP-17, gypenoside XVII; I/R, ischemia and reperfusion; ER, endoplasmic reticulum; H/R, hypoxia/reoxygenation; UPR, unfolded protein response.

dependent manner (2.5, 5, 10, and 20 μM) ($P < 0.05$, $P < 0.01$, or $P < 0.001$). These results illustrate the significant protective effects of GP-17 against H/R injury. Because 20μM and 40 μM GP-17 exhibited similar effects, 20 μM was selected as the optimal concentration for the following experiments.

### 3.2. GP-17 inhibits H/R-induced intracellular ROS accumulation and cell apoptosis

Oxidative damage mediated by free radicals contributes to H/R-induced injury in cardiomyocytes [18]. The ROS ratio was $38.8\% \pm 2.0\%$ in the H/R group versus $26.7\% \pm 1.6\%$ in the control group (Fig. 1F); however, this increase was significantly attenuated by GP-17 preconditioning (Fig. 1F and H; $P < 0.01$).

Antiapoptotic effects of GP-17 were detected by flow cytometry analysis. As shown in Fig. 1I, the percentage of PI-positive cells in the H/R group was significantly higher than the control group ($30.7\% \pm 5.1\%$ versus $12.6\% \pm 3.1\%$, Fig. 1G and I); however, the apoptosis index was significantly decreased by GP-17 in a dose-dependent manner ($P < 0.05$, $P < 0.01$, or $P < 0.001$).

### 3.3. H/R causes severe mitochondrial damage that is inhibited by GP-17 treatment

The changes in mitochondrial membrane potential were assessed by JC-1 staining using a fluorescence microscope. As shown in Fig. 2A and B, H/R treatment significantly decreased the ratio of red to green fluorescence intensity in H9c2 cells ($P < 0.01$). This H/R-induced effect was significantly inhibited by GP-17 pre-conditioning ($P < 0.01$ or $P < 0.001$).

Fig. 2C shows a representative Seahorse experiment, and Fig. 2D represents the statistical analysis of mitochondrial respiration. The cells were evaluated for basal respiration (1−18 min), ATP-linked respiration (18−44 min), maximal respiration (44−79 min) and nonmitochondrial respiration (79−96 min). Compared with the H/R group, the cells in the GP-17−treated groups showed significantly higher levels of maximum uncoupled OCR at P5, P7, and P13. The high-dose of GP-17, especially, significantly enhanced the basal respiration, ATP-linked respiration, maximum respiration, and nonmitochondrial respiration compared with the H/R group (Fig. 2D, all $P < 0.001$). These results provide convincing evidence
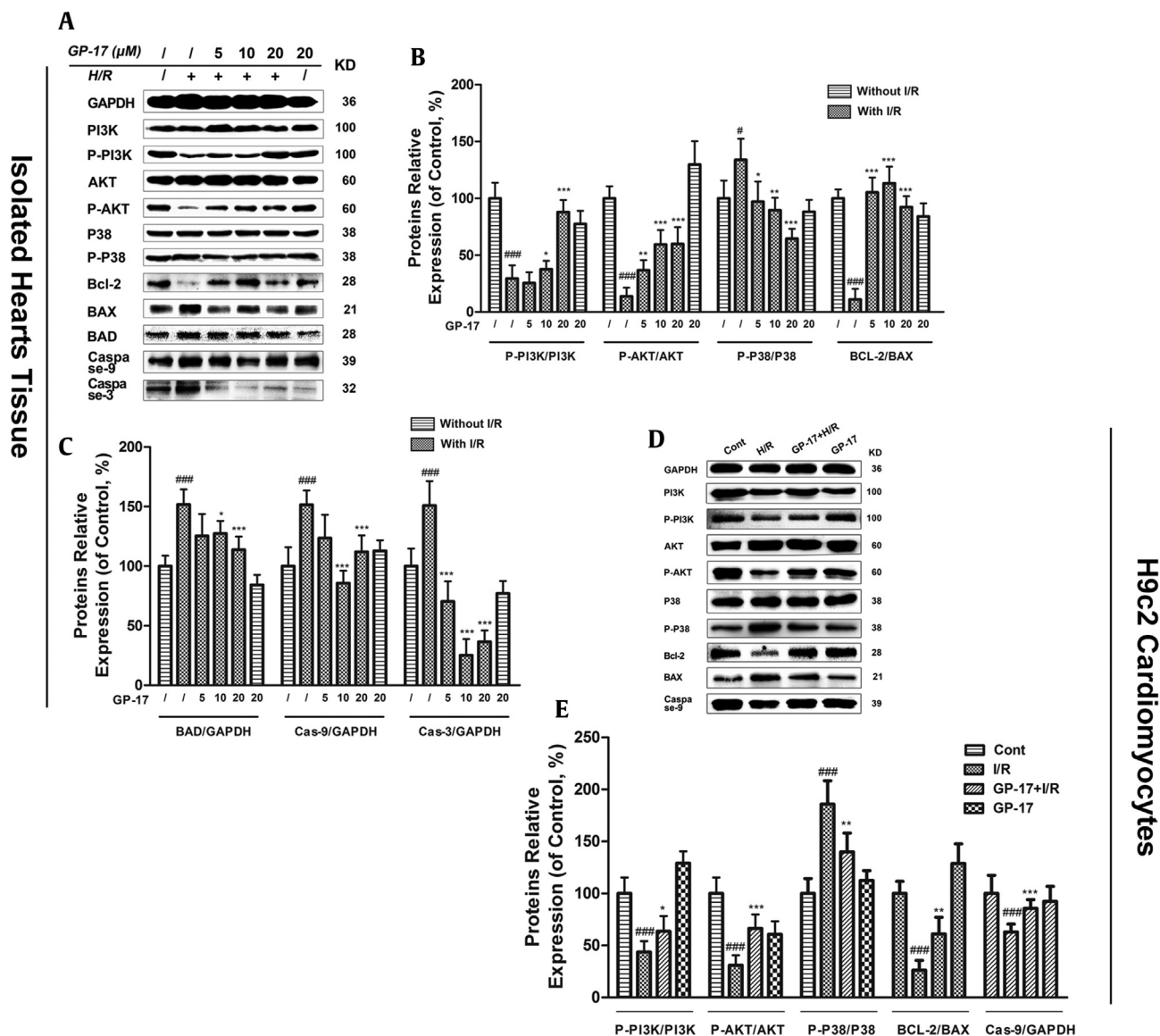
**Fig. 6.** Effects of GP-17 on the protein expression levels of PI3K/AKT and P38 signaling pathways. (A) Immunoblot analysis of P-PI3K, PI3K, P−P38, P38, P-AKT, AKT, Bcl-2, BAX, BAD, caspase-9, caspase-3, and GAPDH were performed in Langendorff rat hearts; (B and C) bar graphs of the proteins' relative expression; (D) immunoblot analysis of P-PI3K, PI3K, P−P38, P38, P-AKT, AKT, Bcl-2, BAX, and caspase-9 were performed in H9c2 cardiomyocytes; (E) bar graphs of the proteins relative expression. #$P < 0.05$ versus the control, ###$P < 0.001$ versus the control, *$P < 0.05$ versus the I/R group, **$P < 0.01$ versus the I/R group, ***$P < 0.001$ versus the I/R group. GP-17, gypenoside XVII; I/R, ischemia and reperfusion.

that GP-17 inhibits cardiomyocyte injury possibly through a mitochondrial-dependent pathway.

### 3.4. GP-17 ameliorates I/R-induced heart dysfunction, suppresses myocardial cell degeneration, and reduces myocardial apoptosis of Langendorff rat hearts

To determine the therapeutic implications of GP-17 on I/R injuries, we used an *ex vivo* Langendorff model. RaH, a calcium uptake inhibitor that functions via a special sodium/calcium channel [19], was used as positive control. The concentrations of GP-17 (5, 10, or 20 μM) dissolved in KH buffer were chosen based on our *in vitro* results and previous experience [4]. After 15 min of stabilization and drug processing, the adult rat hearts were subjected to 40 min of global ischemia and 60 min of reperfusion [4]. At the end of the reperfusion, the LVSP, $+dP/dt_{max}$, and $-dP/dt_{min}$ of the hearts decreased to 46.2%, 51.1%, and 65.3%, respectively, and LVeDP

increased to 395.8% compared with the control group (Fig. 3A, $P < 0.01$ or $P < 0.001$). The impairment function induced by I/R is consistent with the high degree of tissue injury detected by histopathological examination (Fig. 3C) and TUNEL staining (Fig. 3B). The injury, however, was significantly reduced in the GP-17− treated groups. The functional parameters of LVSP and $\pm$ dP/dt in the GP-17 high-dose group demonstrated a near complete recovery, with values of 80.3%, 72.5%, and 89.9% of the levels in the control group, respectively (n = 12, Fig. 3A). LVeDP decreased to 221.7% of that in the control. HR, which was 242.8 $\pm$ 19.7 bpm before ischemia, was not significantly influenced by I/R (Fig. 3A, $P > 0.05$). The results of the histopathological examination confirmed that GP-17 significantly suppressed myocardial cell degeneration, rupture, interstitial edema, and inflammatory cell infiltration induced by I/R (Fig. 3C, $P < 0.05$). TUNEL staining showed that the apoptosis index was markedly increased in the I/R group (Fig. 3B, $P < 0.01$), whereas GP-17 (5, 10, 20 μM) significantly decreased the
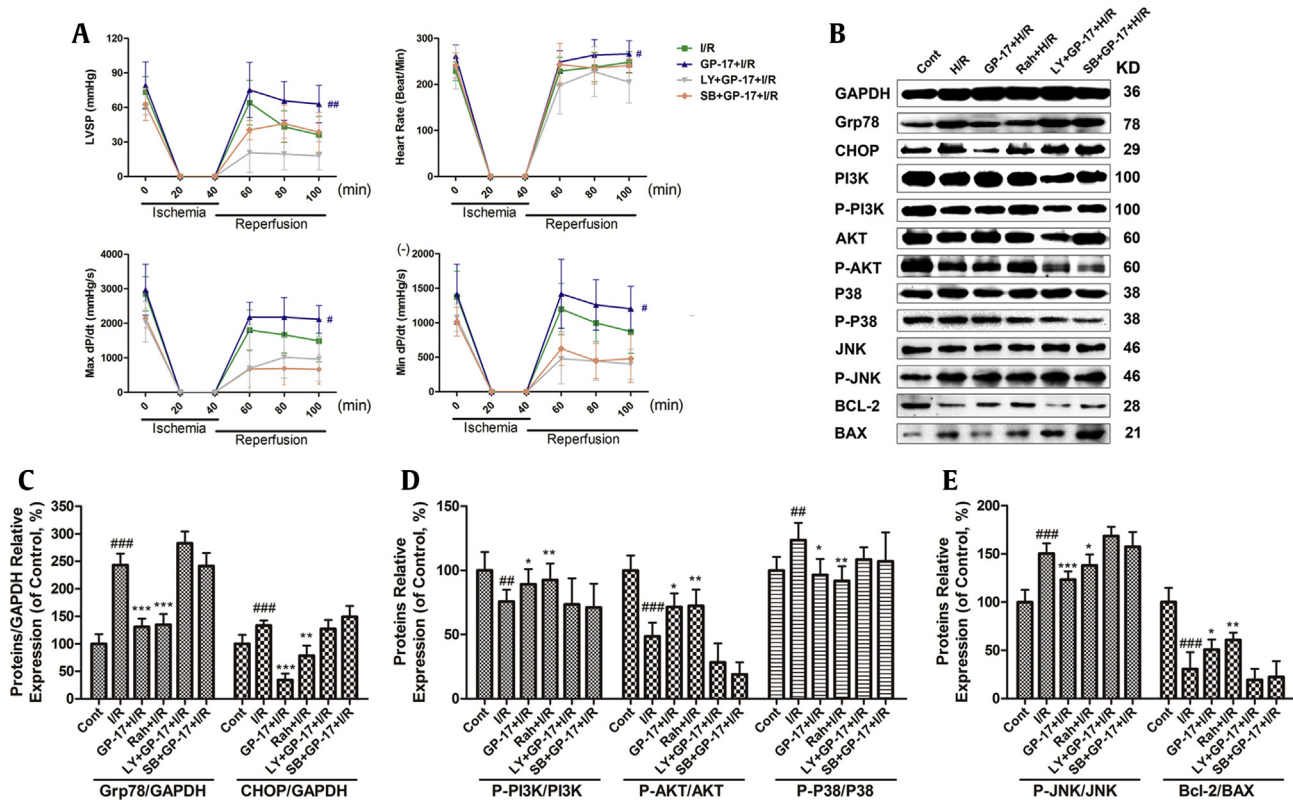
**Fig. 7.** Effects of LY294002 and SB203580 on GP-17−induced cardioprotective effects in Langendorff rat hearts. The hearts with or without 15 min of GP-17 (20μM) preprocessing were exposed to LY or SB for 15 min. (A) The improved function of GP-17 on heart LVSP, LVeDP, heart rate, +dp/dt$_{max}$, and −dp/dt$_{min}$ were suppressed by inhibitors LY and SB; (B) immunoblot analysis of the protein expression levels in Langendorff rat hearts; (C−E) bar graphs showed the relative protein expressions of Grp78, CHOP, PI3K, AKT, P38, JNK, and Bcl-2 were expressed in the [#]$P < 0.05$ versus the control, [##]$P < 0.01$ versus the control, [###]$P < 0.001$ versus the control, [*]$P < 0.05$ versus the I/R group, [**]$P < 0.01$ versus the I/R group, [***]$P < 0.001$ versus the I/R group.
GP-17, gypenoside XVII; LVSP, left ventricular systolic pressure; LVeDP, left ventricular end-diastolic pressure; I/R, ischemia and reperfusion.

apoptosis index compared with the control group. Moreover, 0.3 mM RaH treatment also significantly suppressed the I/R-induced decreases in heart LVSP, +dP/dt$_{max}$, −dP/dt$_{min}$, and increase in LVeDP. Taken together, these results demonstrate that GP-17 ameliorates I/R-induced heart dysfunction in Langendorff rat hearts similar to or better than the RaH-positive control.

### 3.5. GP-17 suppresses oxidative stress in langendorff rat hearts

ROS are disposed enzymatically by CAT, SOD, and GSH-Px depending on the adequate reserves of reduced glutathione [20]. I/R treatment significantly reduced the activities of CAT, SOD, and GSH-Px and enhanced the production of MDA (Fig. 3D, $P < 0.05$ or $P < 0.01$); however, these changes were effectively inhibited by GP-17 pretreatment in a dose-dependent manner, indicating that GP-17 protects the myocardium from I/R injury by altering the activities of antioxidant enzyme.

### 3.6. GP-17 reduces I/R-induced mitochondrial injury and mitochondrial apoptosis

mPTP opening is a major determinant of cell death in the progression of I/R injury [21]. The mitochondria from I/R rats generated significantly more ROS than those from the control rats (Fig. 4A, $P < 0.001$). The significant increase in ROS generation was accompanied by increased levels of mPTP opening (Fig. 4A, $P < 0.001$). Both GP-17 and RaH inhibited ROS generation and mPTP opening. The concentration of Ca$^{2+}$ from the I/R group was significantly reduced as a result of mPTP opening and the inactivation of Ca−Mg-

ATPase (Fig. 4A, $P < 0.01$). GP-17 significantly increased the concentration of Ca$^{2+}$ similar to that in the control group. Interestingly, the protective effects of GP-17 on the mitochondria were significantly suppressed when the inhibitors of Akt (LY) and P38 (SB) were added (Fig. 4A, $P < 0.05$ or $P < 0.01$).

Moreover, the ratio of cytochrome c in the cytosol to that in the mitochondria was significantly higher in the I/R group because of the release of cytochrome c compared with the control (Fig. 4B, $P < 0.01$). Simultaneously, the level of the proapoptotic factor BAX in the I/R group significantly increased; however, the group pretreated with GP-17 (20 μM) showed significantly reduced expression of BAX and release of cytochrome c compared with the I/R group (Fig. 4B and C, $P < 0.05$ or $P < 0.01$).

### 3.7. ER stress is involved in I/R-induced apoptosis and GP-17 inhibits ER stress−associated apoptosis

The ER stress-responsive marker Grp78 and the ER stress sensors activating transcription factor 6 (ATF6), protein kinase RNA-like ER kinase (PERK), eIf2α, and inositol-requiring enzyme 1 (IRE1) [22] were evaluated. As shown in Fig. 5, the expression level of Grp78 was significantly increased in the I/R-treated group by 1.86-fold compared with the control group ($P < 0.01$). In addition, the relative protein expression levels of ATF6, PERK, eIf2α, and IRE1 were significantly increased to varying degrees (1.18-, 1.27-, 1.65- and 1.29-fold compared with the control group, respectively, $P < 0.05$, $P < 0.01$, or $P < 0.001$) in the I/R-treated group. Consistent with previous reports [4], I/R treatment initiated the unfolded protein response (UPR) and ER stress response; however, the GP-17

(5, 10, 20 μM)–treated groups showed a significant reduction in the expression levels of Grp78, PERK, and IRE1, but not in ATF6 (Fig. 5A, C, D, and E, respectively, $P < 0.05$, $P < 0.01$, or $P < 0.001$). The enhanced expression of CHOP, phosphorylated c-Jun N-terminal kinase (P-JNK), and activated caspase-12 are generally related to ER stress [23]. GP-17 (20 μM) significantly suppressed the I/R-induced upregulation of the proapoptotic proteins P-JNK, CHOP, Bad, BAX, and caspase-12 compared with the control group ($P < 0.05$). GP-17 also increased the expression level of the antiapoptotic protein Bcl-2, thereby inhibiting I/R-induced apoptosis. These results indicate that ER stress is involved in I/R-induced myocardial injury and mediates cardiomyocyte apoptosis by PERK/eIF2α- and IRE1-related pathways. More importantly, ER stress and cell apoptosis are markedly suppressed by GP-17 treatment.

### 3.8. The protective role of GP-17 is related to the activation of the PI3K/Akt pathway and the suppression of the P38-MAPK pathway

The PI3K/Akt signaling pathway plays a critical role in cardioprotection in various cardiac disorders [24]. We hypothesized that the PI3K/Akt and P38-MAPK pathways are involved in GP-17–induced cardioprotective effects. To study this question, we performed experiments using the specific PI3K inhibitor, LY, or the P38/MAPK inhibitor, SB. As shown in Fig. 6A and D, decreases in the ratio of p-PI3K/PI3K and p-Akt/Akt and increase in p-P38/P38 were observed in the cells exposed to H/R and in the hearts that underwent I/R; however, pretreatment with LY (6μg/ml) or SB (1 μM) for 15 min reduced the GP-17–enhanced cell resistance to I/R injury. Both LY and SB weakened the beneficial effects of GP-17 on I/R-impaired cardiac dysfunction with regard to LVSP, LVeDP, $+dP/dt_{max}$ and $-dP/dt_{min}$ (Fig. 7A, $P < 0.05$ or $P < 0.01$), but did not significantly affect the HR ($P > 0.05$). LY and SB attenuated the inhibitory effects of GP-17 on ER stress, cytochrome c release, caspase-9/3 activity, and expression of Bcl-2 family proteins (Fig. 7, $P < 0.05$, $P < 0.01$, or $P < 0.001$). Furthermore, LY and SB treatment significantly upregulated the protein expression levels of Grp78 and CHOP compared with the I/R group ($P < 0.05$ or $P < 0.01$), and GP-17 treatment did not affect this overexpression. These results demonstrate that both the PI3K/Akt and P38 signaling pathways are involved in the protective effects of GP-17 against I/R injury.

## 4. Discussion

Myocardial I/R is a complex pathological process involving oxidative stress, ER stress, apoptosis, mitochondrial injury, and myocardial dysfunction [3,25]. In this study, we found that GP-17 reduces cardiac dysfunction, inhibits myocardial oxidative stress and apoptosis, and improves contractile recovery after I/R. We demonstrated that GP-17 reduced I/R-induced mitochondrial injury by delaying the onset of ER stress through the PI3K/AKT and P38 signaling pathways.

GP-17, derived from *Panax notoginseng (Burk.) F. H. Chen*, has been demonstrated to be protective on cerebrovascular and cardiovascular diseases [14]. Here, we explored whether GP-17 provides cardioprotective effects against I/R injury. To address this question, isolated rat hearts under I/R and H9c2 cardiomyocytes subjected to H/R were established to mimic I/R injury *ex vivo* and *in vitro*. Ranolazine·HCL, which is a late sodium channel blocker used for chronic stable angina treatment, was used as a positive control [16]. We observed that GP-17 pretreatment relieved the heart dysfunction caused by I/R (LVSP, LVeDP, $+ dP/dt_{max}$, and $- dP/dt_{min}$) and showed similar or even improved effects compared with the RaH-positive control group. The negligible impairment in the functional parameters of in the GP-17–treated animals is consistent with a significant reduction in tissue injury. The *in vitro* results

confirmed that GP-17 attenuates the inhibitory effects on cell viability, LDH release, and H9c2 cell apoptosis on I/R in a dose-dependent manner.

In I/R cardiomyocytes, oxygen and glucose depletion and increased ROS can induce the UPR and/or ER-associated apoptotic signaling [26,27]. The UPR mediates ER stress through three ER transmembrane receptors: PERK, ATF6, and IRE1α. Prolonged or excessive ER stress would lead to cell death, typically through apoptosis [28]. A recent study reported that the PERK arm of the UPR regulates mitochondrial morphology during acute ER stress [29]. Our data illustrated that I/R markedly increased the levels of the following proteins: ER stress-responsive marker Grp78; ER stress sensors PERK, eIf2α, ATF6, and IRE1; and downstream apoptosis proteins including CHOP, caspase-12, P-JNK, BAX, and Bad. I/R also downregulated Bcl-2, indicating the activation of apoptosis. CHOP is reportedly induced by the PERK/eIF2α-dependent pathway and JNK by the IRE1-mediated pathway [30]. Caspase-12 is a member of the interleukin-1b converting enzyme subfamily and is reported to be specific in ER stress–mediated apoptosis [31]. GP-17 significantly suppressed the I/R-induced processing of caspase-12. When compared with the I/R group, GP-17 pretreatment significantly increased the levels of Bcl-2 and decreased the expression of ER stress–responsive proteins and apoptosis proteins, especially those involved in the PERK/eIF2α and IRE1-related pathways. Together these results demonstrate that GP-17 can prevent I/R-initiated ER stress and cell apoptosis.

The ER-mitochondria junction and it's function in cell death have received recent increasing attention [32,33]. Targeting mitochondria, ER, or both may be possible strategies for the protection of cardiac diseases. With recent developments in the Seahorse XF Extracellular Flux Analyzer, we are able to assess intact cell bioenergetic profiles in real time [34]. The popular label-free system can evaluate a cell's two major energy-producing pathways simultaneously, namely, mitochondrial respiration (oxygen consumption) and glycolysis (extracellular acidification) [35]. Our results indicated that GP-17 significantly enhanced the basal respiration, ATP-linked respiration, maximum respiration, and nonmitochondrial respiration compared with the H/R group. The *ex vivo* results confirmed that GP-17 inhibited the generation of ROS and mPTP opening in the mitochondria from I/R rats. The concentration of $Ca^{2+}$ from the I/R mitochondria significantly decreased as a result of mPTP opening and inactivation of Ca–Mg-ATPase. A large ROS burst and $[Ca^{2+}]i$ overload on reperfusion of an ischemic heart are major triggers for mPTP opening [36]. MPTP allows solutes and water to enter the mitochondria, which increases the matrix volume and causes mitochondrial outer membrane rupture. GP-17 significantly increased the activities of CAT, SOD, and GSH-Px a and reduced the production of MDA in I/R-perfused rat hearts in a dose-dependent manner, indicating that GP-17 inhibits oxidative stress by enhancing the activities of antioxidant enzymes.

The PI3K/Akt signaling pathway promotes cardioprotection in many cardiac diseases [37]. The activation of P38/mammalian target of rapamycin is important in various heart diseases [38]. We tested whether the PI3K/Akt and P38-MAPK pathways took part in GP-17–induced cardioprotection through the use of specific inhibitors. Our results indicate that preconditioning with LY or SB dramatically decreased GP-17–improved cell resistance to I/R injury. LY and SB impaired the beneficial effects of GP-17 on ER stress, caspase-9/3 activity, cytochrome c release, and activation of apoptosis-associated proteins. These results suggest that GP-17 protects cardiomyocytes against I/R injury via suppressing the PI3K/AKT- and P38-mediated ER stress signaling pathways.

## 5. Conclusion

The results of this study elucidate the significant protective effects of GP-17 against I/R injuries both *ex vivo* and in vitro; such effects were mediated partly by suppressing ER stress–induced mitochondrial injuries through PI3K/AKT and P38-related signaling pathways. The effects of GP-17 on the alleviation of ER stress and mPTP opening are associated with the inhibition of oxidative stress. However, the overall mechanisms underlying the cardioprotective effects of GP-17 and its association with ER stress and mitochondrial damage must be further investigated.

## Declaration of competing interest

All authors have no conflicts of interest to declare.

## Acknowledgments

## Appendix A. Supplementary data

Supplementary data to this article can be found online at https://doi.org/10.1016/j.jgr.2019.09.003.

## References

[1] Johnson JA, Cavallari LH. Pharmacogenetics and cardiovascular disease–implications for personalized medicine. Pharmacological Reviews 2013 Jul;65(3):987–1009. PubMed PMID: 23686351. Pubmed Central PMCID: 3698938.

[2] Duehrkop C, Rieben R. Ischemia/reperfusion injury: effect of simultaneous inhibition of plasma cascade systems versus specific complement inhibition. Biochemical Pharmacology 2014 Mar 1;88(1):12–22. PubMed PMID: 24384116.

[3] Logue SE, Gustafsson AB, Samali A, Gottlieb RA. Ischemia/reperfusion injury at the intersection with cell death. Journal of Molecular and Cellular Cardiology 2005 Jan;38(1):21–33. PubMed PMID: 15623419.

[4] Yu Y, Sun G, Luo Y, Wang M, Chen R, Zhang J, Ai Q, Xing N, Sun X. Cardioprotective effects of Notoginsenoside R1 against ischemia/reperfusion injuries by regulating oxidative stress- and endoplasmic reticulum stress-related signaling pathways. Scientific Reports 2016;6:21730. PubMed PMID: 26888485. Pubmed Central PMCID: 4757886.

[5] Chan JY, Biden TJ, Laybutt DR. Cross-talk between the unfolded protein response and nuclear factor-kappaB signalling pathways regulates cytokine-mediated beta cell death in MIN6 cells and isolated mouse islets. Diabetologia 2012 Nov;55(11):2999–3009. PubMed PMID: 22893028.

[6] Sozen E, Karademir B, Ozer NK. Basic mechanisms in endoplasmic reticulum stress and relation to cardiovascular diseases. Free Radical Biology & Medicine 2015 Jan;78C:30–41. PubMed PMID: 25452144.

[7] Dejeans N, Tajeddine N, Beck R, Verrax J, Taper H, Gailly P, Calderon PB. Endoplasmic reticulum calcium release potentiates the ER stress and cell death caused by an oxidative stress in MCF-7 cells. Biochemical Pharmacology 2010 May 1;79(9):1221–30. PubMed PMID: 20006589.

[8] Prola A, Nichtova Z, Da Silva JP, Piquereau J, Monceaux K, Guilbert A, Gressette M, Ventura-Clapier R, Garnier A, Zahradnik I, et al. ER stress induces cardiac dysfunction through architectural modifications and alteration of mitochondrial function in cardiomyocytes. Cardiovascular Research 2018. cvy197-cvy.

[9] Giorgi C, Missiroli S, Patergnani S, Duszynski J, Wieckowski MR, Pinton P. Mitochondria-associated membranes: composition, molecular mechanisms, and physiopathological implications. Antioxidants & Redox Signaling 2015 Apr 20;22(12):995–1019. PubMed PMID: 25557408.

[10] Dorn 2nd GW. Mitochondrial dynamism and heart disease: changing shape and shaping change. EMBO Molecular Medicine 2015 Jul;7(7):865–77. PubMed PMID: 25861797. Pubmed Central PMCID: 4520653.

[11] Ong SB, Samangouei P, Kalkhoran SB, Hausenloy DJ. The mitochondrial permeability transition pore and its role in myocardial ischemia reperfusion injury. Journal of Molecular and Cellular Cardiology 2015 Jan;78:23–34. PubMed PMID: 25446182.

[12] Sun J, Sun G, Meng X, Wang H, Wang M, Qin M, Ma B, Luo Y, Yu Y, Chen R, et al. Ginsenoside RK3 prevents hypoxia-reoxygenation induced apoptosis in H9c2 cardiomyocytes via AKT and MAPK pathway. Evidence-based complementary and alternative medicine. eCAM 2013;2013:690190. PubMed PMID: 23935671. Pubmed Central PMCID: 3712237.

[13] Han SY, Li HX, Ma X, Zhang K, Ma ZZ, Jiang Y, Tu PF. Evaluation of the anti-myocardial ischemia effect of individual and combined extracts of Panax notoginseng and Carthamus tinctorius in rats. Journal of Ethnopharmacology 2013 Feb 13;145(3):722–7. PubMed PMID: 23237935.

[14] Meng X, Wang M, Sun G, Ye J, Zhou Y, Dong X, Wang T, Lu S, Sun X. Attenuation of Abeta25-35-induced parallel autophagic and apoptotic cell death by gypenoside XVII through the estrogen receptor-dependent activation of Nrf2/ARE pathways. Toxicology and Applied Pharmacology 2014 Aug 15;279(1):63–75. PubMed PMID: 24726523.

[15] Meng X, Luo Y, Liang T, Wang M, Zhao J, Sun G, Sun X. Gypenoside XVII enhances lysosome biogenesis and autophagy Flux and accelerates autophagic clearance of amyloid-beta through TFEB activation. Journal of Alzheimer's Disease : JAD 2016 Apr 5. PubMed PMID: 27060963.

[16] Rosano GM, Vitale C, Volterrani M. Pharmacological management of chronic stable Angina: focus on ranolazine. Cardiovascular Drugs and Therapy 2016 Aug;30(4):393–8. PubMed PMID: 27417323.

[17] Krebs J, Agellon LB, Michalak M. Ca(2+) homeostasis and endoplasmic reticulum (ER) stress: an integrated view of calcium signaling. Biochemical and Biophysical Research Communications 2015 Apr 24;460(1):114–21. PubMed PMID: 25998740.

[18] Liu CW, Yang F, Cheng SZ, Liu Y, Wan LH, Cong HL. Rosuvastatin post-conditioning protects isolated hearts against ischemia-reperfusion injury: the role of radical oxygen species, PI3K-Akt-GSK-3beta pathway and mitochondrial permeability transition pore. Cardiovascular Therapeutics 2016 Aug 31. PubMed PMID: 27580017.

[19] Pulford BR, Kluger J. Ranolazine therapy in cardiac arrhythmias. Pacing and clinical electrophysiology. PACE 2016 Sep;39(9):1006–15. PubMed PMID: 27358212.

[20] Palencia G, Medrano JA, Ortiz-Plata A, Farfan DJ, Sotelo J, Sanchez A, Trejo-Solis C. Anti-apoptotic, anti-oxidant, and anti-inflammatory effects of thalidomide on cerebral ischemia/reperfusion injury in rats. Journal of the Neurological Sciences 2015 Apr 15;351(1–2):78–87. PubMed PMID: 25818676.

[21] Horstkotte J, Perisic T, Schneider M, Lange P, Schroeder M, Kiermayer C, Hinkel R, Ziegler T, Mandal PK, David R, et al. Mitochondrial thioredoxin reductase is essential for early postischemic myocardial protection. Circulation 2011 Dec 20;124(25):2892–902. PubMed PMID: 22144571.

[22] McLaughlin M, Vandenbroeck K. The endoplasmic reticulum protein folding factory and its chaperones: new targets for drug discovery? British Journal of Pharmacology 2011 Jan;162(2):328–45. PubMed PMID: 20942857. Pubmed Central PMCID: 3031055.

[23] Li H, Zhu X, Fang F, Jiang D, Tang L. Down-regulation of GRP78 enhances apoptosis via CHOP pathway in retinal ischemia-reperfusion injury. Neuroscience Letters 2014 Jul 11;575:68–73. PubMed PMID: 24880098.

[24] Dong M, Hu N, Hua Y, Xu X, Kandadi MR, Guo R, Jiang S, Nair S, Hu D, Ren J. Chronic Akt activation attenuated lipopolysaccharide-induced cardiac dysfunction via Akt/GSK3beta-dependent inhibition of apoptosis and ER stress. Biochimica et Biophysica Acta 2013 Jun;1832(6):848–63. PubMed PMID: 23474308. Pubmed Central PMCID: 3653446.

[25] Ferdinandy P, Hausenloy DJ, Heusch G, Baxter GF, Schulz R. Interaction of risk factors, comorbidities, and comedications with ischemia/reperfusion injury and cardioprotection by preconditioning, postconditioning, and remote conditioning. Pharmacological Reviews 2014 Oct;66(4):1142–74. PubMed PMID: 25261534.

[26] Yuan Y, Guo Q, Ye Z, Pingping X, Wang N, Song Z. Ischemic postconditioning protects brain from ischemia/reperfusion injury by attenuating endoplasmic reticulum stress-induced apoptosis through PI3K-Akt pathway. Brain Research 2011 Jan 7;1367:85–93. PubMed PMID: 20940001.

[27] Yu L, Lu M, Wang P, Chen X. Trichostatin A ameliorates myocardial ischemia/reperfusion injury through inhibition of endoplasmic reticulum stress-induced apoptosis. Archives of Medical Research 2012 Apr;43(3):190–6. PubMed PMID: 22564421.

[28] Urra H, Dufey E, Lisbona F, Rojas-Rivera D, Hetz C. When ER stress reaches a dead end. Biochimica et biophysica acta 2013 Dec;1833(12):3507–17. PubMed PMID: 23988738.

[29] Lebeau J, Saunders JM, Moraes VWR, Madhavan A, Madrazo N, Anthony MC, Wiseman RL. The PERK arm of the unfolded protein response regulates mitochondrial morphology during acute endoplasmic reticulum stress. Cell Reports 2018 Mar 13;22(11):2827–36. PubMed PMID: 29539413. Pubmed Central PMCID: 5870888.

[30] Marwarha G, Dasari B, Ghribi O. Endoplasmic reticulum stress-induced CHOP activation mediates the down-regulation of leptin in human neuroblastoma SH-SY5Y cells treated with the oxysterol 27-hydroxycholesterol. Cellular Signalling 2012 Feb;24(2):484–92. PubMed PMID: 21983012. Pubmed Central PMCID: 3237961.

[31] Kadowaki H, Nishitoh H, Ichijo H. Survival and apoptosis signals in ER stress: the role of protein kinases. Journal of Chemical Neuroanatomy 2004 Sep;28(1–2):93–100. PubMed PMID: 15363494.

[32] Bagur R, Tanguy S, Foriel S, Grichine A, Sanchez C, Pernet-Gallay K, Kaambre T, Kuznetsov AV, Usson Y, Boucher F, et al. The impact of cardiac ischemia/reperfusion on the mitochondria-cytoskeleton interactions. Biochimica et Biophysica Acta 2016 Jun;1862(6):1159–71. PubMed PMID: 26976332.

[33] Bernard-Marissal N, Medard JJ, Azzedine H, Chrast R. Dysfunction in endoplasmic reticulum-mitochondria crosstalk underlies SIGMAR1 loss of function mediated motor neuron degeneration. Brain : A Journal of Neurology 2015 Apr;138(Pt 4):875–90. PubMed PMID: 25678561.

[34] Lange M, Zeng Y, Knight A, Windebank A, Trushina E. Comprehensive method for culturing embryonic dorsal root ganglion neurons for Seahorse extracellular Flux XF24 analysis. Frontiers in Neurology 2012;3:175. PubMed PMID: 23248613. Pubmed Central PMCID: 3522103.

[35] Rogers GW, Brand MD, Petrosyan S, Ashok D, Elorza AA, Ferrick DA, Murphy AN. High throughput microplate respiratory measurements using minimal quantities of isolated mitochondria. PloS One 2011;6(7):e21746. PubMed PMID: 21799747. Pubmed Central PMCID: 3143121.

[36] Yan XH, Guo XY, Jiao FY, Liu X, Liu Y. Activation of large-conductance Ca(2+)-activated K(+) channels inhibits glutamate-induced oxidative stress through attenuating ER stress and mitochondrial dysfunction. Neurochemistry International 2015 Nov;90:28–35. PubMed PMID: 26163046.

[37] Cuadrado-Berrocal I, Gomez-Gaviro MV, Benito Y, Barrio A, Bermejo J, Fernandez-Santos ME, Sanchez PL, Desco M, Fernandez-Aviles F, Fernandez-Velasco M, et al. A labdane diterpene exerts ex vivo and in vivo cardioprotection against post-ischemic injury: involvement of AKT-dependent mechanisms. Biochemical Pharmacology 2014 Dec 31. PubMed PMID: 25557296.

[38] Sun GB, Sun H, Meng XB, Hu J, Zhang Q, Liu B, Wang M, Xu HB, Sun XB. Aconitine-induced Ca2+ overload causes arrhythmia and triggers apoptosis through p38 MAPK signaling pathway in rats. Toxicology and Applied Pharmacology 2014 Aug 15;279(1):8–22. PubMed PMID: 24840785.